TWO-COLOR TEMPERATURE MEASUREMENT METHOD USING BPW34 PIN PHOTODIODES

I. Bonefačić[*] – P. Blecich

Faculty of Engineering, University of Rijeka, Vukovarska 58, 51000 Rijeka, Croatia

Abstract:

This work presents a simple and inexpensive technique for non-contact industrial temperature measurements based on the two-color method. Since non-contact temperature measurements require expensive instruments such as IR cameras or ratio pyrometers, a simple ratio pyrometer consisting of only two BPW34 PIN photodiodes with narrowband filters is introduced. Temperature measurements using this instrument are carried out on a muffle furnace and are verified with thermal imaging camera - FLIR Thermacam S65. Temperatures measured with both instruments are in good accordance. This method using only two photodiodes presents a reliable and cost effective alternative for temperature measurements and flame monitoring where high temperatures are expected and non-contact measurement is required, such as in industrial furnaces, gasifiers or internal combustion engines.

1   Introduction

Heat sources emit light as a function of temperature. It is possible to acquire the image to get total temperature distribution. If an image of a source can be acquired, post-processing techniques can be developed to calculate the source temperature. In the area of non-contact temperature measurement, the techniques developed and used are based on the two-colour radiation thermometry. The traditional pyrometers determine the temperature based on a single wavelength and the emissivity value of the surface.

However, the emissivity information is too complicated to calculate since the actual surface conditions may not be known or the emissivity may be varying with the temperature of the object itself, which is why they are not accurate enough for measuring the temperature in the furnace. The two-colour pyrometer (also called ratio pyrometer) measures the temperature independent of emissivity, hence, more and more researchers are interested in applying this technique in the industry. Basically, this type of instrument uses the ratio of two spectral radiances measured over two different wavelengths to determine the true temperature.

Hottel and Broughton [1] invented the two-colour method in 1932. They attempted to measure the true temperature and total radiation from the luminous gas flame in the furnace. Application of the method has been expanded over years to soot temperature measurements and flame monitoring [2], in various applications such as combustion engines [3,4], coal burners [5,6], and industrial furnaces and gasifiers [7,8]. It is also applicable to metallurgy where temperature field is a crucial factor for a successful

[*] Corresponding author. Tel.: +385 51 651 561
E-mail address: igorb@riteh.hr

process but the experimental methods for testing the distribution and change of the temperature field have been inadequate [9]. Digital still cameras have gained significant popularity in recent years. The development of digital cameras has opened up possibilities for powerful new diagnostic techniques employing two-dimensional imaging based on two-colour radiation thermometry [10-12]. Digital photography is a fast measurement technique and requires no other sensors. But IR cut filter and RGB matrix placed directly on the sensor limit its use in temperature measurement. Although useful for everyday imaging, camera image processing has problems that cannot be solved without reverse engineering. Using simple photodiodes as sensors, which are not limited by those factors, temperature measurement of full spectrum radiation sources can be measured in real time with high precision at a fraction of the cost. As the temperature can be measured only at one point at the time, this method is not capable of fully replacing digital still cameras for two-dimensional thermal imaging, although the resolution can be improved by using multiple sensors simultaneously.

2   Measurement principle

A blackbody radiator emits a continuous stream of thermal radiation from its surface. This radiation forms a continuous spectrum though the intensity varies throughout the spectrum. The irradiance E_λ at any wavelength λ throughout the spectrum depends only on the blackbody temperature and increases with its temperature. These relationships are quantitatively embodied in Planck's law of blackbody radiation [13]:

$$E_\lambda(T) = \frac{C_1}{\lambda^5}\left(e^{C_2/\lambda T} - 1\right)^{-1}, \qquad (1)$$

where C_1 and C_2 are constants defined as $2 \cdot h \cdot c^2$ and $h \cdot c/k$ respectively, where h is Planck's constant, c is speed of light in vacuum and k is Boltzmann's constant. For short wavelengths i.e., $\lambda \ll C_2/T$ and the temperatures below 3000 K, the Planck function can be replaced by the Wien approximation:

$$\left(e^{C_2/\lambda T} - 1\right)^{-1} \approx e^{-C_2/\lambda T}, \qquad (2)$$

i.e., the Plank's radiant law, Eq. (1), can be replaced by the Wien radiant law:

$$E_\lambda(T) = \frac{C_1}{\lambda^5} e^{-C_2/\lambda T}. \qquad (3)$$

Eq. (3) is used for an idealized black body. However, the furnace environment acts as a gray body. According to [14], over a wavelength range from 200 to 1100 nm, the gasoline flame can be assumed to be a gray body in the range from 550 nm to 900 nm and for the coal-fired flame, the range is between 500 nm and 1000 nm. So, an additional term for emissivity ε_λ, at the given wavelength, must be added in the equation.

$$E_\lambda(T) = \varepsilon_\lambda \frac{C_1}{\lambda^5} e^{-C_2/\lambda T}. \qquad (4)$$

If the spectral irradiances $E_{\lambda 1}(T)$ and $E_{\lambda 2}(T)$ are calculated simultaneously, at wavelengths λ_1 and λ_2 as:

$$E_{\lambda 1}(T) = \varepsilon_{\lambda 1} \frac{C_1}{\lambda_1^5} e^{-C_2/\lambda_1 T}, \qquad (5)$$

$$E_{\lambda 2}(T) = \varepsilon_{\lambda 2} \frac{C_1}{\lambda_2^5} e^{-C_2/\lambda_2 T}, \qquad (6)$$

their ratio is as follows:

$$\frac{E_{\lambda 1}(T)}{E_{\lambda 2}(T)} = \frac{\varepsilon_{\lambda 1} \dfrac{C_1}{\lambda_1^5} e^{-C_2/\lambda_1 T}}{\varepsilon_{\lambda 2} \dfrac{C_1}{\lambda_2^5} e^{-C_2/\lambda_2 T}}. \qquad (7)$$

The ratio is proportional to the signals detected by photodiodes $L_{\lambda 1}(T)$, $L_{\lambda 1}(T)$, under the wavelengths λ_1 and λ_2:

$$\frac{E_{\lambda 1}(T)}{E_{\lambda 2}(T)} = A \cdot \frac{L_{\lambda 1}(T)}{L_{\lambda 2}(T)}. \qquad (8)$$

The correction coefficient A in Eq. (8), is influenced by many factors, such as spectral sensitivity $S(\lambda)$ of the photodiode, transmission of narrowband filters τ, measurement noise [15] etc. Derived from Eq. (7) and Eq. (8), the temperature can be determined as:

$$T = \frac{C_2\left(\dfrac{1}{\lambda_2} - \dfrac{1}{\lambda_1}\right)}{\ln\dfrac{L_{\lambda 1}(T)}{L_{\lambda 2}(T)} + \ln A - \ln\left(\dfrac{\varepsilon_{\lambda 1}}{\varepsilon_{\lambda 2}}\right) - 5\ln\left(\dfrac{\lambda_2}{\lambda_1}\right)} \quad (9)$$

If λ_1 and λ_2 are relatively close, then it can be assumed that $\varepsilon_{\lambda 1} \approx \varepsilon_{\lambda 2}$ and Eq. (9) is simplified to:

$$T = \frac{C_2\left(\dfrac{1}{\lambda_2} - \dfrac{1}{\lambda_1}\right)}{\ln\dfrac{L_{\lambda 1}(T)}{L_{\lambda 2}(T)} + \ln A - 5\ln\left(\dfrac{\lambda_2}{\lambda_1}\right)} \quad (10)$$

Eq. (10) is the basic equation of the two-color method temperature measurement. In order to obtain the value of correction coefficient A, many methods have been proposed by recent researchers. Lu et al. [16] employed the tungsten lamp as a standard temperature source for calibration. The calibration process needs the true temperature of the tungsten lamp and also assumes that filament emissivity at different points of the lamp is identical. This results in some errors in the temperature distribution measurement. Two methods are proposed and applied to the experiment, [11]: the former named *reference method* based on the known temperature of the reference body; the latter named *response curve method* where A is calculated from the photodiode relative spectral sensitivity curve and transmission coefficients of chosen narrowband filters.

2.1 Reference method

This method is based on the known temperature of the reference body which is regarded as the reference region. Based on the known temperature T_{known} and detected signals from reference region $L_{\lambda 1}$ and $L_{\lambda 2}$, the correction coefficient can be calculated from Eq. (11):

$$A_{\text{ref}} = \frac{L_{\lambda 2}}{L_{\lambda 1}} \cdot \left(\frac{\lambda_2}{\lambda_1}\right)^5 \cdot e^{\frac{C_2\left(\frac{1}{\lambda_2} - \frac{1}{\lambda_1}\right)}{T_{known}}} \quad (11)$$

The main disadvantage of the reference method is its dependence on the reference region temperature measurement accuracy.

2.2 Response curve method

This method is based on the relationship between the photodiode response S and source radiance E. The photodiode response is represented by the relative spectral sensitivity curve and the source radiance is indicated by the detected signal on the photodiode. When transmission and FWHM (*Full Width at Half Maximum*) of narrowband filters are known, the detected signals at wavelengths λ_1 and λ_2 become [15]:

$$L_{\lambda 1}(T) = \int_{\lambda_{1L}}^{\lambda_{1H}} S(\lambda) \cdot E(\lambda,T) \cdot \tau_1(\lambda) \cdot d\lambda \quad (12)$$

$$L_{\lambda 2}(T) = \int_{\lambda_{2L}}^{\lambda_{2H}} S(\lambda) \cdot E(\lambda,T) \cdot \tau_2(\lambda) \cdot d\lambda \quad (13)$$

where ranges from λ_{1L} to λ_{1H} and λ_{2L} to λ_{2H} are transmission ranges of the narrowband filters. The ratio of $L_{\lambda 1}(T)$ and $L_{\lambda 2}(T)$ is:

$$\frac{L_{\lambda 1}(T)}{L_{\lambda 2}(T)} = \frac{\int_{\lambda_{1L}}^{\lambda_{1H}} S(\lambda) \cdot E(\lambda,T) \cdot \tau_1(\lambda) \cdot d\lambda}{\int_{\lambda_{2L}}^{\lambda_{2H}} S(\lambda) \cdot E(\lambda,T) \cdot \tau_2(\lambda) \cdot d\lambda} \quad (14)$$

For narrowband filters where FWHM is small, Eq. (14) could be simplified to:

$$\frac{L_{\lambda 1}(T)}{L_{\lambda 2}(T)} = \frac{S(\lambda_1) \cdot E(\lambda_1,T) \cdot \tau_1}{S(\lambda_2) \cdot E(\lambda_2,T) \cdot \tau_2}, \quad (15)$$

where $S(\lambda_1)$ and $S(\lambda_2)$ are relative spectral sensitivities of the photodiode at chosen wavelengths, τ_1 and τ_2 are transmission of narrowband filters at those wavelengths. From Eq. (8) and Eq. (15) the correction coefficient can be calculated as:

$$A_{\text{resp}} = \frac{S(\lambda_2) \cdot \tau_2}{S(\lambda_1) \cdot \tau_1}. \quad (16)$$

For higher temperatures as in furnaces, measurement wavelengths below 3000 nm are advantageous to obtain large signal ratios and to minimize the influence of the reflected background radiation [17].

PIN photodiode BPW34 has sensitivity curve which falls below 1000 nm with its peak at about 900 nm, Fig 1. Two narrowband filters with FWHM of 10 nm at wavelengths 860 nm and 970 nm are selected.

Wavelengths are chosen to be in the region of the greatest sensitivity of the photodiode based on the relative spectral sensitivity curve. Transmission curves of chosen narrowband filters obtained from manufacturer ("PixelTeq") are presented in Fig. 2.
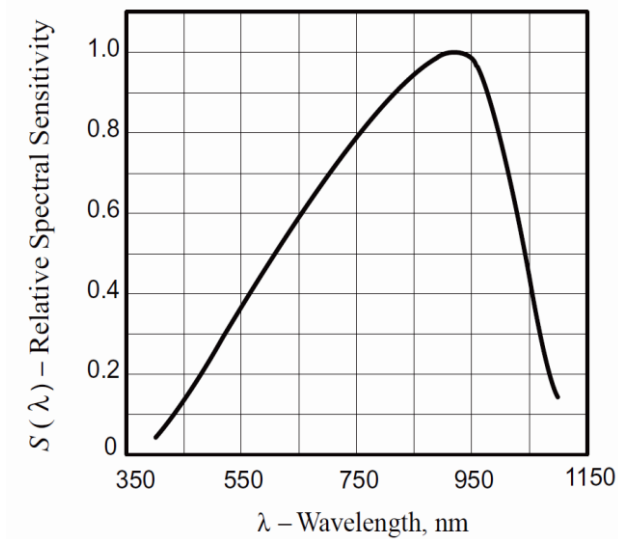

Figure 1. Relative spectral sensitivity of BPW34 photodiode [18].
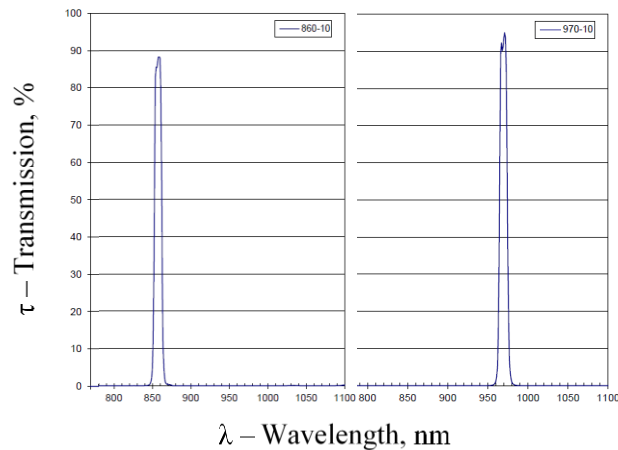

Figure 2. Transmission curves of narrowband filters [18].

Based on photodiode relative spectral sensitivity curve and transmission curves of chosen narrowband filters, the correction coefficient can be determined from Eq. (16):

$$A_{\text{resp}} = \frac{S(\lambda_2) \cdot \tau_2}{S(\lambda_1) \cdot \tau_1} = \frac{0{,}93 \cdot 0{,}92}{0{,}95 \cdot 0{,}86} = 1{,}0472 \ . \quad (17)$$

This method depends entirely on data accuracy provided by manufacturers of photodiodes and narrowband filters but it does not demand any kind of additional calibration measurements.

3 Temperature measurements

It is not possible to directly measure the spectral irradiance using photodiodes at any given wavelength. However, its intensity is proportional to the generated photocurrent in the photodiode, i.e., reverse light current I_{ra} in Fig. 3, which can be calculated from the measured voltage, V_{out}:

$$V_{\text{out}} = (I_0 + I_{\text{ra}}) \cdot R_{\text{L}} \quad (18)$$

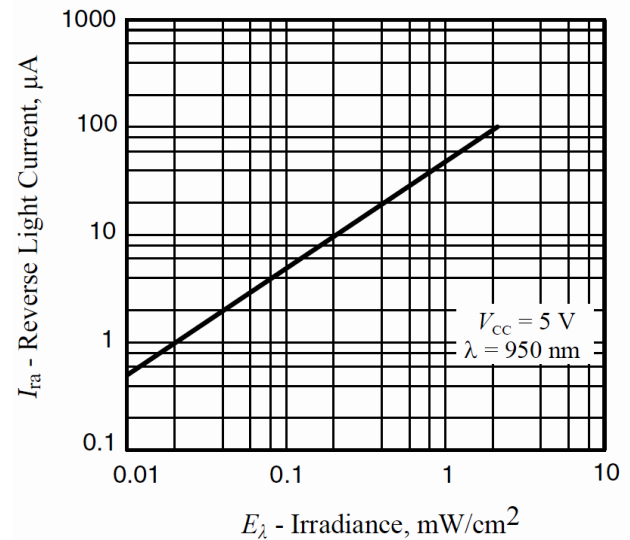where R_{L} is known load resistance and I_0 is dark current.

Figure 3. Reverse light current vs. Irradiance [18].

Photodiodes generate current due to the photovoltaic effect so they can operate without the need for external power source. However, frequency response and linearity can be improved by using an external reverse bias voltage. While application of a reverse voltage to a photodiode is very useful as stated before, it has accompanying disadvantage of increasing dark current and noise levels along with the danger of damaging the device by applying excessive reverse voltage. Chosen photodiode provides not only good response speed but excellent dark current and voltage resistance with reverse voltage applied [18].

Reverse biasing the photodiode with voltage V_{CC} enables photodiode to work in photoconductive mode. Fig. 4 shows basic circuitry (A) and load line (B) for photoconductive mode of operation.
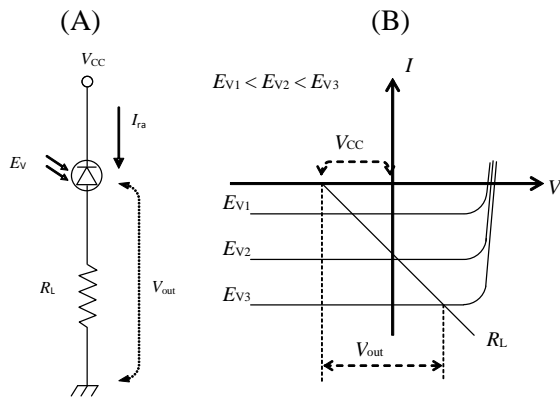

Figure 4. Photodiode in photoconductive mode.

Measuring voltages, i.e., generated photocurrent of two separate photodiodes irradiated at different wavelengths, as in schematics in Fig. 5, the ratio $L_{\lambda 1}/L_{\lambda 2}$ in Eq. (15) can be determined as:

$$\frac{L_{\lambda 1}}{L_{\lambda 2}} = \frac{V_1}{V_2} . \tag{19}$$
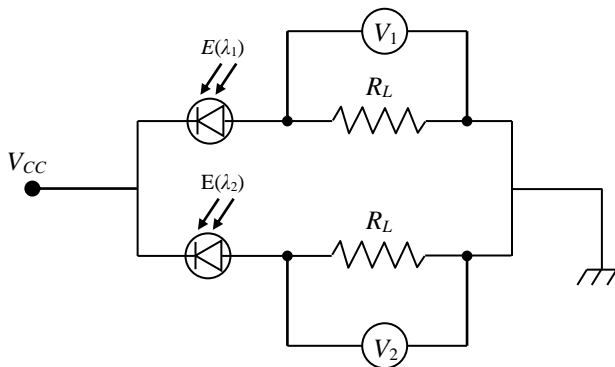

Figure 5. Schematic diagram of temperature measurement setup.

Knowing the correction coefficient determined previously by response curve method, Eq. (17), temperature can be obtained from Eq. (10) and Eq. (19):

$$T_{\text{resp}} = \frac{C_2\left(\dfrac{1}{\lambda_2} - \dfrac{1}{\lambda_1}\right)}{\ln\dfrac{V_1}{V_2} + \ln A_{\text{resp}} - 5\ln\left(\dfrac{\lambda_2}{\lambda_1}\right)} . \tag{20}$$

Voltages V_1 and V_2 were measured using 16 bit ADC (analog-to-digital converter) ADS1115 from "Texas Instruments Inc." [19] connected to the Arduino microcontroller for data logging. Before actual measurements, the calibration of the ADC was performed consisting of 100 measurements with covered sensor (dark frames), which were averaged and later subtracted from actual measurements to cancel offset error and thermal noise. Also, special attention was paid to the effect of stray light which could cause significant errors during temperature measurements.

4 Furnace temperature measurement

Temperature measurements were carried out on the laboratory muffle furnace with the temperature control up to 1200 °C. Sensor with photodiodes was placed approximately 50 cm in front of the chamber opening (Fig. 6). Temperature of the furnace was set in steps at 800 °C, 900 °C, 950 °C, 1000 °C, 1050 °C and 1100 °C and the chamber temperature was monitored with thermal imaging camera FLIR ThermaCAM S65 (Fig. 7). The door of the chamber was opened after each temperature setting was reached and measurements were carried out simultaneously with photodiode sensor and thermal camera. Every second, sensor data was sent to the Arduino microcontroller equipped with SD memory card for data logging. Measurement results are presented on the diagram in Fig. 8 and Table 1.

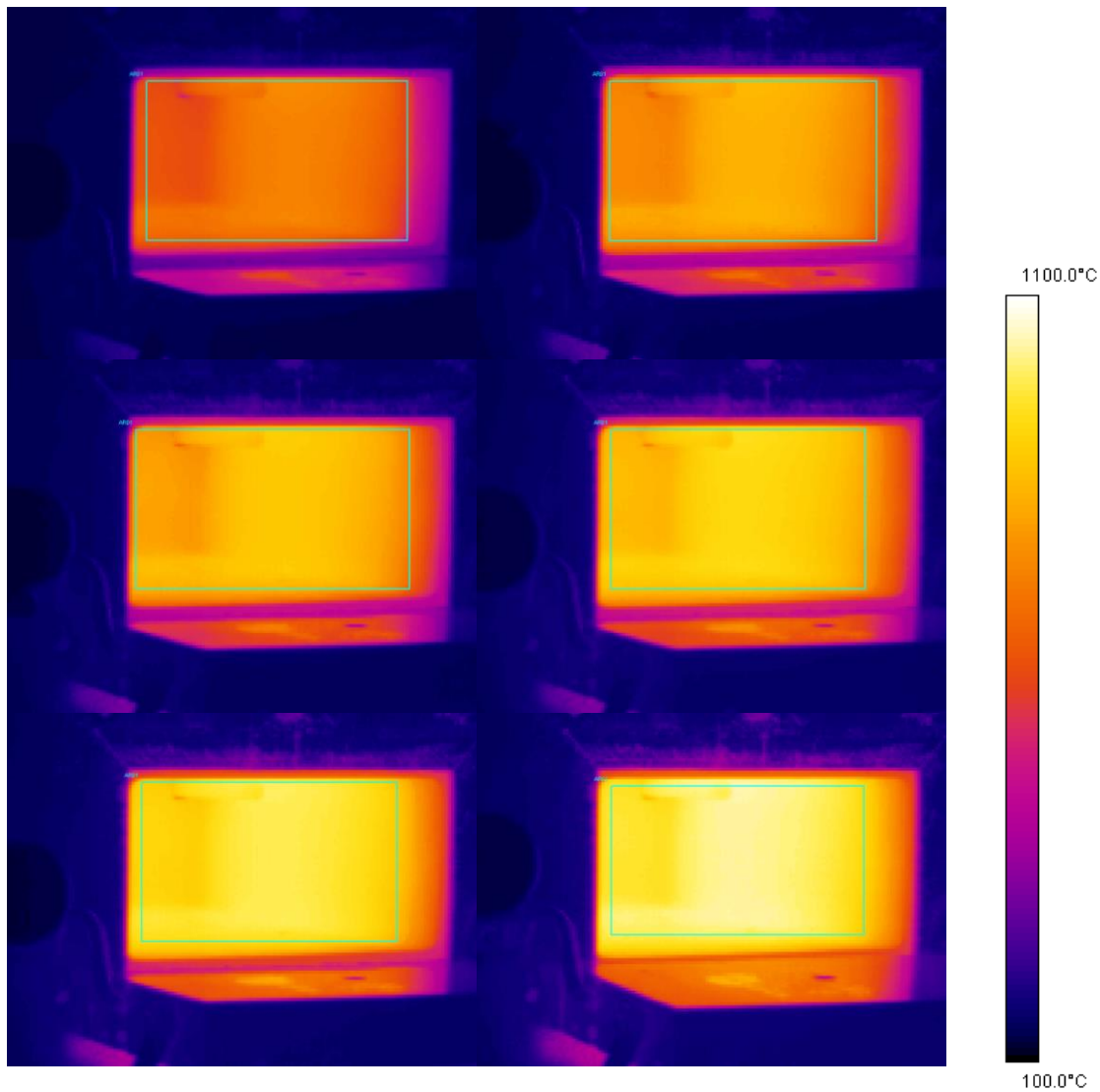*Figure 6. Temperature sensor and the muffle furnace.*

_____

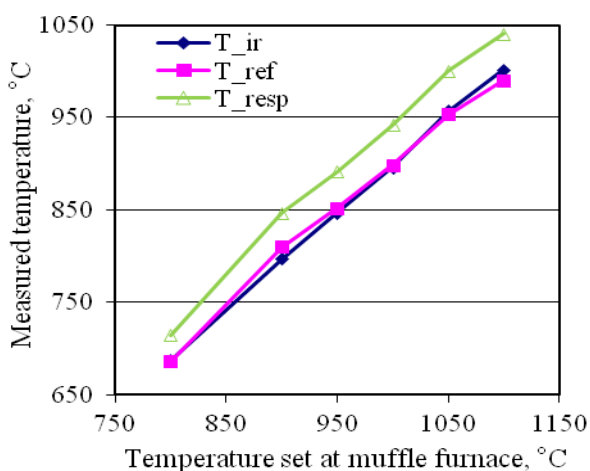*Figure 7. Thermograms of the muffle furnace set at 800 °C, 900 °C, 950 °C, 1000 °C, 1050 °C and 1100 °C.*

Figure 8. Muffle furnace temperature measurements.

Green line in Fig. 8 represents temperature measurements (T_{resp}) using the correction coefficient calculated by the response curve method (A_{resp}=1.0472). As can be seen from Table 1, measured values are as much as 50 °C higher than values obtained with IR camera (blue line). If temperatures measured with IR camera T_{IR} are used as reference values, and by minimizing RMS error between measured temperatures (T_{IR}) and temperatures calculated from Eq. (10), optimized correction coefficient based on reference temperatures, $A_{ref,opt}$=0.9876, could be obtained. Temperatures measured using optimized correction coefficient (T_{ref}) are presented with magenta line in Fig. 8. It could be seen from Table 1 that temperature difference measured with reference method is less than 2% of T_{IR}. The response curve

Table 1. Results of temperature measurements with two-color method using photodiodes

FLIR ThermaCAM S65	Measured voltages		Two-color method		Temperature difference, %	
T_{IR}, °C	V_1, mV	V_2, mV	T_{resp}, °C	T_{ref}, °C	Response curve method	Reference method
687	3.76	15.14	715	686	3.9	0.2
797	16.18	51.70	847	810	5.9	1.6
847	48.67	145.53	891	852	5.0	0.6
896	64.31	179.48	942	899	4.9	0.3
957	114.57	296.97	1001	954	4.4	0.4
1002	198.92	492.45	1041	990	3.7	1.2

method, on the other hand, gives less satisfactory temperature values, which can be related to data inaccuracy provided by manufacturers of photodiodes and/or narrowband filters.

5 Conclusion

We presented a method of radiation thermometry using a pair of PIN photodiodes. Our system uses the submicron wavelength, which makes the temperature measurement less influenced by errors than when performed with thermal infrared wavelengths (>3000 nm). As a result of the calibration experiment, sensor consisting from a pair of BPW34 PIN photodiodes with narrowband filters using the near-infrared wavelength of about 1000 nm is proven to be applicable to temperature measurements in the temperature range from 800 °C to 1100 °C. Theoretically, higher temperatures could also be measured with the same accuracy but that was not verified due to the limited maximum temperature achievable by the muffle furnace. Lower temperatures, however, could not be measured because generated photocurrent was too small to be precisely measured with ADS1115, analog to digital converter. It could be done by using more complex circuitry or more expensive ADC but the intention here was to use simple components and keep the costs as low as possible.

Because of its non-intrusive nature and relative ease of the application, this method is suitable for industrial furnaces where continuous and reliable in-flame temperature measurements are necessary.

References

[1] Hottel, H. C., Broughton, F. P.: *Determination of true temperature and total radiation from luminous gas flames,* Industrial and Engineering Chemistry (Analytical Edition), 4 (1932), 2, 166-175.

[2] Berry Yelverton, T. L., Roberts, E. L.: *Soot surface temperature measurements in pure and diluted flames at atmospheric and elevated pressures*, Experimental Thermal and Fluid Science, 33 (2008), 1, 17-22.

[3] Mancaruso, E., Vaglieco, B. M: *Optical investigation of the combustion behaviour inside the engine operating in HCCI mode and using alternative diesel fuel*, Experimental Thermal and Fluid Science, 34 (2010), 3, 346-351.

[4] Cheng, X., Chen, L., Yan, F., Dong, S.: *Study on soot formation characteristics in the diesel combustion process based on an improved detailed soot*, Energy Conversion and Management, 75 (2013), 1-10.

[5] Jiang, Z. W., Luo, Z. X., Zhou, H. C.: *A simple measurement method of temperature and emissivity of coal-fired flames from visible radiation image and its application in a CFB boiler furnace*, Fuel, 88 (2009), 980-987.

[6] Draper, T. S., Zeltner, D., Tree, D. R., Xue, Y., Tsiava, R.: *Two-dimensional flame temperature and emissivity measurements of pulverized oxy-coal flames*, Applied Energy, 95 (2012), 38-44.

[7] Chen, J., Osborn, P., Paton, A., Wall, P.: *CCD Near Infrared Temperature Imaging in the Steel Industry*, Industrial and Measurement Technology Conference, Irvane, CA, USA, 1993, 299-303.

[8] Yan, Z., Liang, Q., Guo, Q., Yu, G., Yu, Z.: *Experimental investigations on temperature distributions of flame sections in a bench-scale opposed multi-burner gasifier*, Applied Energy, 86 (2009), 1359-1364.

[9] Lu, J., Sun, B., Tang, F., Ding, T., Zhang, L.: Numerical simulation of temperature field of

plasma ARC remelting on EN-SGJ-600-3, Engineering Review, 33 (2013), 2, 115-121.

[10] Panditrao, M., Rege, P. P.: *Estimation of furnace temperature distribution using digital photographic images*, Association of Metallurgical Engineers of Serbia, AMES, 15 (2009), 2, 115-123.

[11] Li, D.: *Thermal image analysis using calibrated video imaging*, PhD Thesis, University of Missouri, Columbia, May 2006.

[12] Zhao, H., Feng, H., Xu, Z., Li, Q.: *Research on temperature distribution of combustion flames based on high dynamic range imaging*, Optics & Laser Technology, 39 (2007), 1351-1359.

[13] Planck, M.: *On the Law of the Energy Distribution in the Normal Spectrum*, Annals of Physics, 4 (1901), 3, 553-563.

[14] Sun, Y., Lou, C., Zhou, H.: *A simple judgment method of gray property of flames based on spectral analysis and the two-color method for measurements of temperatures and emissivity*, Proceedings of the Combustion Institute, 33 (2011), 1, 735-741.

[15] Macdonald, L.W., Luo, M. R.: *Colour Imaging - Vision and Technology*, John Wiley & Sons Ltd, England, 1999.

[16] Lu, G., Yan, Y., Riley, G., Bheemul, H. C.: *Concurrent Measurement of Temperature and Soot Concentration of Pulverized Coal Flames*, IEEE 112 Transactions on Instrumentation and Measurement, 51 (2002), 5, 990-995.

[17] Möllmann, K. P., Pinno, F., Vollmer, M.: *Two-Color or Ratio Thermal Imaging – Potentials and Limits*, Application Note for Research & Science, FLIR Technical Series, University of Applied Sciences, Brandenburg, Germany, 2011.

[18] BPW34 silicon PIN diode, Vishay Semiconductors, http://www.vishay.com/docs/81521/bpw34.pdf

[19] ADS1115, Analog-to-digital converter, Texas Instruments, http://www.ti.com/lit/ds/symlink/ads1115.pdf